JOURNAL OF THEORETICAL
AND APPLIED MECHANICS
48, 3, pp. 677-701, Warsaw 2010

ANALYSIS OF MOVEMENT OF THE BOP CRANE UNDER SEA WEAVING CONDITIONS

Andrzej Urbaś
Marek Szczotka
Andrzej Maczyński

University of Bielsko-Biala, Faculty of Management and Computer Science, Bielsko-Biała, Poland
e-mail: aurbas@ath.bielsko.pl; mszczotka@ath.bielsko.pl; amaczynski@ath.bielsko.pl

In the paper, mathematical models for dynamic analysis of a BOP crane under sea weaving conditions are presented. The BOP crane is a kind of gantry crane. It is installed on drilling platforms and used for transportation of the Blowout Preventor (BOP). The most important features characterising its dynamics are: motion of the crane base caused by sea weaving, clearance in the supporting system (between the support and rails), impacts of the load into guides and a significant weight of the load. In order to investigate dynamics of the system, its mathematical model taking into consideration all these features has been formulated. Equations of motions have been derived using homogenous transformations. In order to improve numerical effectiveness of the model, the equations have been transformed to an explicit form. The input in the drive of the travel system has been modelled in two ways: the kinematic input via a spring-damping element and the force input. Exemplary results of numerical calculations are presented.

Key words: modelling, dynamic analysis, BOP crane

1. Introduction

The exploitation of undersea oil and natural gas pools is one of the fastest growing fields of economy. In view of specific environmental conditions, technical instruments used in this branch of industry need to fulfil specific exceptional requirements. These instruments are called the offshore equipment, while the whole section of engineering concerning this field is known as the offshore technology. The motion of a base of offshore instruments is the most characteristic feature of the offshore engineering. A vital problem faced by researchers who wish to perform calculations of offshore equipment dynamics is how to describe this motion. The principal factor here is the sea waving which is a very complex phenomenon. For analysis of certain offshore equipment, particularly cranes, an assumption is often made that the ship moves only in the vertical plane coincident with the transversal symmetry axis of its deck. Sinusoidal waves of angular frequency 0.56 and 0.74 $\mathrm{rad\,s^{-1}}$ and height 1 m propagating along the ship transversal axis were assumed in Das and Das (2005). In Balachandran *et al.* (1999) two kinds of functions describing motion of the on-board crane jib sheave have been used. They were harmonic and pseudo-harmonic functions. Masoud (2000) assumed swaying and surging oscillations as well as heaving, pitching and rolling of a ship with a crane installed on board. Calculations were based on empirically measured data from Fossen (1994) covering swaying and surging oscillations and heaving motion of a chosen point of the ship (reference point). Also Driscoll *et al.* (2000) used measured vertical dislocations of an A-frame to investigate the model of a cage suspended at considerable depths. The additional loads caused by wind, impact of floe or ice field, hoarfrost, sea currents and many others usually not occurring in the land technology also need to be taken into account (Handbook of Offshore Engineering, 2005).

Cranes are an important kind of offshore devices. There are many publications concerning their dynamics and control. Ellermann and Kreuzer (2003) investigated the influence of a mooring system on the dynamics of a crane. Jordan and Bustamante (2007), Maczyński and Wojciech (2008) analysed the taut-slack phenomenon.

Motion of offshore crane bases cause the load to significantly sway even when the crane does not execute any working movements. There are papers concerning methods of stabilisation of the load positioning for offshore cranes – Cosstick (1996), Birkeland (1998), Pedrazzi and Barbieri (1998), Li and Balachandran (2001), Maczyński and Wojciech (2007). More bibliographical information concerning offshore cranes and motion of their bases can be found in Maczyński (2006).

One of the types of offshore cranes is a BOP crane. The construction of Protea from Gdańsk is presented in Fig. 1a. It is a gantry crane installed on a drilling platform designed to transport a system of valves named BOP (Blowout Preventor). The BOP is used to block an uncontrolled outflow of oil or natural gas from a wellbore at the seabed. After drilling the wellbore, the BOP is put inside it and afterwards the risers are being connected to the BOP. The risers drain off oil or gas into suitable tanks. In view of the plug task, weight of the BOP reaches hundreds of tons. During the transportation process (during the travel of a gantry crane) the BOP is protected by a system of guides presented in Fig. 1b.

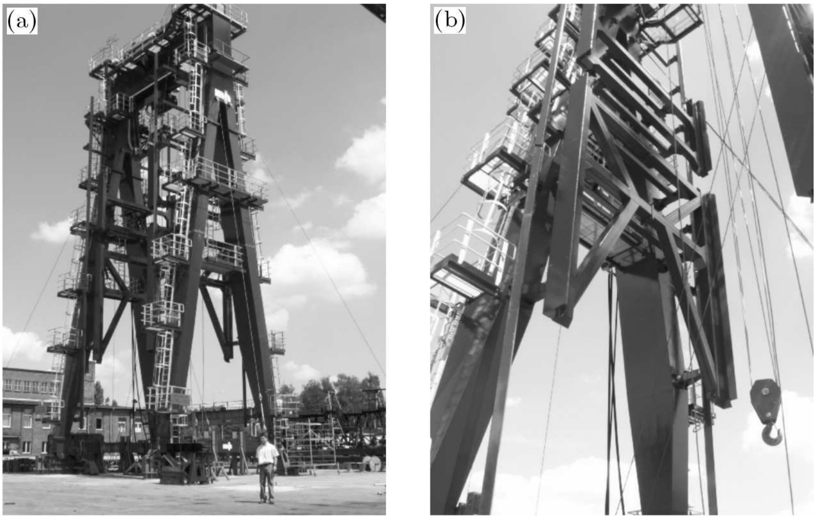

Fig. 1. (a) BOP crane, (b) guide system

The clearance between the load and the guide system equals a few centimeters. The weight of the presented crane is 200 T, hoisting capacity 550 T and height about 30 m. The BOP cranes are hardly ever a topic of scientific papers.

The analysis of a travel system is an interesting and important problem concerning the dynamics of a BOP crane. The crane is supported on rails and its motion is realised by means of a rack and a toothed wheel – Fig. 2a. The maximum velocity of travel of the crane is equal to 3 m/min. Due to the movement of the platform deck caused by sea weaving and wind forces, protection systems are used. These systems limit the movement of the crane in the vertical and horizontal direction, perpendicular to the longitudinal axis of the rails. This task is particularly realised by an anti-lift system presented in Fig. 2b.

When the drive system of the crane is being designed, the dynamic forces should be taken into consideration despite the insignificant velocity of crane travel. The dynamic forces can be critical for some reasons:

- significant weight of the moving crane,
- general motion of the deck caused by sea weaving,
- clearance in the anti-lift system,
- additional dynamic forces generated by the load impact against the guides.

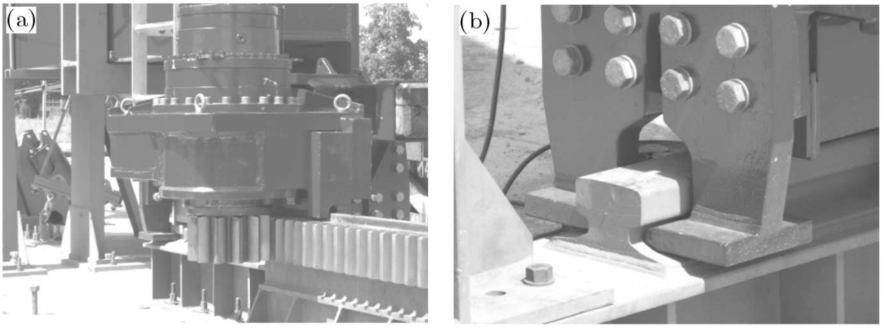

Fig. 2. (a) Rack travel system, (b) anti-lift system

In the paper, preliminary results of the dynamic analysis of the drive system of the BOP crane are presented. In the mathematical model, all the aforementioned features are taken into consideration.

2. The dynamic model of a BOP crane

The mathematical model of the system has been formulated to enable dynamic analysis of the BOP crane, see Urbaś and Wojciech (2008, 2009). In these papers, general relations concerning the equations of crane motion are presented. In our work, we have derived formulas describing Lagrange operators in an explicit form. It is important due to convenience of numerical calculations. Furthermore, we have evolved more accurate models of the drivers of the travel system of the BOP crane.

The schema of the model of the BOP crane together with more important coordinate systems is presented in Fig. 3.

The following basic assumptions for modelling are established:

- motion of the base (system $\{D\}$) is known and described by functions

$$\begin{array}{lll} x^{(D)} = x^{(D)}(t) & y^{(D)} = y^{(D)}(t) & z^{(D)} = z^{(D)}(t) \\ \psi^{(D)} = \psi^{(D)}(t) & \theta^{(D)} = \theta^{(D)}(t) & \varphi^{(D)} = \varphi^{(D)}(t) \end{array} \tag{2.1}$$

- structure of the crane (frame) is treated as a rigid body – it should be noticed that the construction of the BOP crane is a kind of combination of two A-frames; the A-frame has been a subject of many analyses presented by Fałat (2004) which proved that the influence of flexibility of

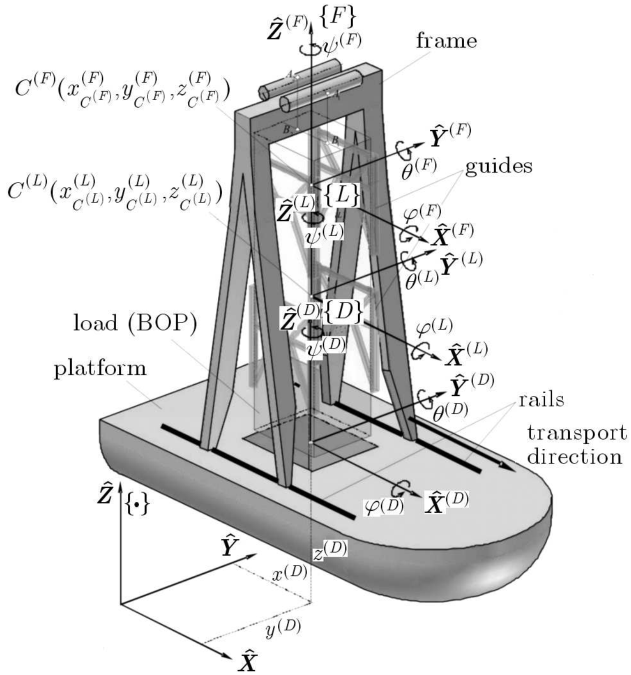

Fig. 3. Schema of the BOP crane model

the frame on dynamics of the whole system (on motion of the load) is slight,

- load is a rigid body of a rectangular shape,
- load is suspended on two ropes – their flexibility and damping are taken into account,
- load can touch the guides only along its edges,
- clearance and flexibility between the load and guides are taken into consideration,
- frame is mounted flexibly to the deck and, additionally, in the $\widehat{\boldsymbol{Y}}^{(D)}$ direction a clearance can occur,
- input in the drive system has been modelled in two ways: kinematic input via a spring-damping element and force input,
- wind force can be taken into consideration,
- homogenous transformations are used to describe the system geometry (Wittbrodt *et al.*, 2006).

Both the load (system $\{L\}$ in Fig. 3) and the frame (system $\{F\}$) have 6 degrees of freedom with respect to the deck (system $\{D\}$). So, the model has 12 degrees of freedom and the vector of generalised coordinates has the following form

$$\boldsymbol{q} = \begin{bmatrix} \boldsymbol{q}^{(F)} \\ \boldsymbol{q}^{(L)} \end{bmatrix} \tag{2.2}$$

where

$$\begin{aligned} \boldsymbol{q}^{(F)} &= [x^{(F)}, y^{(F)}, z^{(F)}, \psi^{(F)}, \theta^{(F)}, \varphi^{(F)}]^\top \\ \boldsymbol{q}^{(L)} &= [x^{(L)}, y^{(L)}, z^{(L)}, \psi^{(L)}, \theta^{(L)}, \varphi^{(L)}]^\top \end{aligned}$$

Equations of motion of the system have been derived from Lagrange equations of the second kind

$$\frac{d}{dt}\frac{\partial E}{\partial \dot{q}_k} - \frac{\partial E}{\partial q_k} + \frac{\partial V}{\partial q_k} + \frac{\partial D}{\partial \dot{q}_k} = Q_k \qquad k = 1, \dots, 12 \tag{2.3}$$

where E is the kinetic energy of the system, V – potential energy, D – function of energy dissipation, Q_k – non-potential generalised force corresponding to the coordinate k, q_k – element of the vector $\boldsymbol{q}$.

In the next sections, the features of the BOP crane that potentially have bigger influence on the dynamics of the drive system are described in greater detail.

2.1. Motion of the base of the BOP crane – the system $\{D\}$

It has been mentioned that motion of the base (deck of the platform), that means motion of the system $\{D\}$, with respect to the deck has been assumed as known. It is described by pseudo-harmonic functions

$$y_i^{(D)} = \sum_{j=1}^{n_i^{(D)}} A_{i,j}^{(D)} \sin(\omega_{i,j}^{(D)} t + \varphi_{i,j}^{(D)}) \qquad i = 1, \dots, 6 \tag{2.4}$$

where $A_{i,j}^{(D)}$, $\omega_{i,j}^{(D)}$, $\varphi_{i,j}^{(D)}$ denote the amplitude, angular frequency and phase angle of the input, respectively, $n_i^{(D)}$ – number of harmonics in the series.

The application of homogenous transformations (Wittbrodt *et al.*, 2006) allows one to convert the position vector of the point defined in the system $\{D\}$ to system $\{\cdot\}$ according to relation

$$\boldsymbol{r}_P^{\{\cdot\}} = \mathbf{T}^{(D)} \boldsymbol{r}_P^{\{D\}} \tag{2.5}$$

where $\boldsymbol{r}_p^{\{\cdot\}} = [x_p, y_p, z_p, 1]^\top$ is the position vector of the point P in the system $\{\cdot\}$, $\boldsymbol{r}_P^{\{D\}} = [x_P^{\{D\}}, y_P^{\{D\}}, z_P^{\{D\}}, 1]^\top$ – position vector of the point P in the system $\{D\}$, $\mathbf{T}^{(D)}$ – matrix of homogenous transformation from the system $\{D\}$ to the system $\{\cdot\}$.

Matrix $\mathbf{T}^{(D)}$ can be presented as the product of six matrices where each of them is a function of one variable dependent on time

$$\mathbf{T}^{(D)}(t) = \mathbf{T}_1^{(D)}\mathbf{T}_2^{(D)}\mathbf{T}_3^{(D)}\mathbf{T}_6^{(D)}\mathbf{T}_5^{(D)}\mathbf{T}_4^{(D)} \tag{2.6}$$

and according to Fig. 3

$$\mathbf{T}_1^{(D)} = \mathbf{T}_1^{(D)}(x^{(D)}) = \begin{bmatrix} 1 & 0 & 0 & x^{(D)} \\ 0 & 1 & 0 & 0 \\ 0 & 0 & 1 & 0 \\ 0 & 0 & 0 & 1 \end{bmatrix}$$

$$\mathbf{T}_2^{(D)} = \mathbf{T}_2^{(D)}(y^{(D)}) = \begin{bmatrix} 1 & 0 & 0 & 0 \\ 0 & 1 & 0 & y^{(D)} \\ 0 & 0 & 1 & 0 \\ 0 & 0 & 0 & 1 \end{bmatrix}$$

$$\mathbf{T}_3^{(D)} = \mathbf{T}_3^{(D)}(z^{(D)}) = \begin{bmatrix} 1 & 0 & 0 & 0 \\ 0 & 1 & 0 & 0 \\ 0 & 0 & 1 & z^{(D)} \\ 0 & 0 & 0 & 1 \end{bmatrix}$$

$$\mathbf{T}_4^{(D)} = \mathbf{T}_4^{(D)}(\varphi^{(D)}) = \begin{bmatrix} 1 & 0 & 0 & 0 \\ 0 & c\varphi^{(D)} & -s\varphi^{(D)} & 0 \\ 0 & s\varphi^{(D)} & c\varphi^{(D)} & 0 \\ 0 & 0 & 0 & 1 \end{bmatrix}$$

$$\mathbf{T}_5^{(D)} = \mathbf{T}_5^{(D)}(\theta^{(D)}) = \begin{bmatrix} c\theta^{(D)} & 0 & s\theta^{(D)} & 0 \\ 0 & 1 & 0 & 0 \\ -s\theta^{(D)} & 0 & c\theta^{(D)} & 0 \\ 0 & 0 & 0 & 1 \end{bmatrix}$$

$$\mathbf{T}_6^{(D)} = \mathbf{T}_6^{(D)}(\psi^{(D)}) = \begin{bmatrix} c\psi^{(D)} & -s\psi^{(D)} & 0 & 0 \\ s\psi^{(D)} & c\psi^{(D)} & 0 & 0 \\ 0 & 0 & 1 & 0 \\ 0 & 0 & 0 & 1 \end{bmatrix}$$

and

$$x^{(D)} = x^{(D)}(t) = y_1^{(D)} \qquad y^{(D)} = y^{(D)}(t) = y_2^{(D)}$$
$$z^{(D)} = z^{(D)}(t) = y_3^{(D)} \qquad \varphi^{(D)} = \varphi^{(D)}(t) = y_4^{(D)}$$
$$\theta^{(D)} = \theta^{(D)}(t) = y_5^{(D)} \qquad \psi^{(D)} = \psi^{(D)}(t) = y_6^{(D)}$$
$$s\alpha = \sin\alpha \qquad c\alpha = \cos\alpha$$

The order of rotations included in the matrix $\mathbf{T}^{(D)}$ is agreeable with Euler angles ZYX.

2.2. Kinetic and potential energy of the frame and load

The application of equations (2.3) requires the definition of relations describing kinetic and potential energy of bodies composing the analysed system – in this case the energy of the frame and the load. One of the ways of calculation of kinetic energy of a rigid body is the usage of formula (Wittbrodt *et al.*, 2006)

$$E = \frac{1}{2}\int_m \mathrm{tr}\,(\dot{\boldsymbol{r}}\dot{\boldsymbol{r}}^\top)\,dm = \frac{1}{2}\,\mathrm{tr}\,\{\dot{\mathbf{T}}\mathbf{H}\dot{\mathbf{T}}^\top\} \tag{2.7}$$

where $\boldsymbol{r}$ is the position vector of the point P in the system $\{\cdot\}$, m – mass of the rigid body, $\mathbf{T}$ – transformation matrix to the system $\{\cdot\}$, $\mathbf{H}$ – pseudo-inertia matrix the form of which is inter alia given in Wittbrodt *et al.* (2006).

Introducing the notion of Lagrange operator

$$\varepsilon_k = \frac{d}{dt}\frac{\partial E}{\partial \dot{q}_k} - \frac{\partial E}{\partial q_k} \tag{2.8}$$

where k is the number of the generalised coordinate, and using the transformation presented by Wittbrodt *et al.* (2006), one can obtain a short form

$$\varepsilon_k = \mathrm{tr}\,\{\mathbf{T}_k\mathbf{H}\ddot{\mathbf{T}}^\top\} = \sum_{i=1}^n a_{k,i}\ddot{q}_i + \sum_{i=1}^n\sum_{j=1}^n \mathrm{tr}\,\{\mathbf{T}_k\mathbf{H}\mathbf{T}_{i,j}^\top\}\dot{q}_i\dot{q}_j \tag{2.9}$$

where

$$\mathbf{T}_k = \frac{\partial \mathbf{T}}{\partial q_k} \qquad \mathbf{T}_{i,j} = \frac{\partial^2 \mathbf{T}}{\partial q_i \partial q_j} \qquad a_{k,i} = \mathrm{tr}\,\{\mathbf{T}_k\mathbf{H}\mathbf{T}_i^\top\}$$

The notation (2.9) has been used in many publications, e.g. Maczyński and Wojciech (2003), Adamiec-Wójcik *et al.* (2008). However, as far as the efficiency of numerical calculations is concerned, the notation is not the most profitable. It requires repeated multiplication of matrices of 4×4 dimension and then calculation of the trace of the resultant matrices. In this work, the authors decided to derive formulae describing Lagrange operators in an explicit form. An important feature of a rotational matrix, that is its orthogonality, has been used.

If one denotes the homogenous transformation matrix from the frame system $\{F\}$ to the deck system $\{D\}$ as $\widetilde{\mathbf{T}}^{(F)}$ and from the load system $\{L\}$ as $\widetilde{\mathbf{T}}^{(L)}$, the transformation matrices from the frame system and from the load system to the system $\{\cdot\}$ can be calculated as

$$\mathbf{T}^{(F)} = \mathbf{T}^{(D)}\widetilde{\mathbf{T}}^{(F)} \qquad \mathbf{T}^{(L)} = \mathbf{T}^{(D)}\widetilde{\mathbf{T}}^{(L)} \tag{2.10}$$

Next, the transformations have a universal character and they are not dependent on the local coordinate system. Therefore, instead of equations (2.10) we will use one general formula

$$\mathbf{T} = \mathbf{T}^{(D)}\widetilde{\mathbf{T}} \tag{2.11}$$

Time derivatives of the transformation matrix $\mathbf{T}$ are

$$\dot{\mathbf{T}} = \dot{\mathbf{T}}^{(D)}\widetilde{\mathbf{T}} + \mathbf{T}^{(D)}\dot{\widetilde{\mathbf{T}}} \qquad \ddot{\mathbf{T}} = \dot{\mathbf{T}}^{(D)}\widetilde{\mathbf{T}} + 2\dot{\mathbf{T}}^{(D)}\dot{\widetilde{\mathbf{T}}} + \dot{\mathbf{T}}^{(D)}\ddot{\widetilde{\mathbf{T}}} \tag{2.12}$$

so, relation (2.9) can be presented in the following form

$$\begin{aligned}\varepsilon_k = {} & \mathrm{tr}\Big\{\mathbf{T}^{(D)}\widetilde{\mathbf{T}}_k\mathbf{H}\big[\ddot{\mathbf{T}}^{(D)}\widetilde{\mathbf{T}} + 2\dot{\mathbf{T}}^{(D)}\dot{\widetilde{\mathbf{T}}} + \mathbf{T}^{(D)}\ddot{\widetilde{\mathbf{T}}}\big]^\top\Big\} = \\ = {} & \underbrace{\mathrm{tr}\,\{\mathbf{T}^{(D)^\top}\mathbf{T}^{(D)}\widetilde{\mathbf{T}}_k\mathbf{H}\ddot{\widetilde{\mathbf{T}}}^\top\}}_{\varepsilon_{k,2}} + \underbrace{\mathrm{tr}\,\{\ddot{\mathbf{T}}^{(D)^\top}\mathbf{T}^{(D)}\widetilde{\mathbf{T}}_k\mathbf{H}\widetilde{\mathbf{T}}^\top\}}_{\varepsilon_{k,0}} + \\ & +2\,\underbrace{\mathrm{tr}\,\{\dot{\mathbf{T}}^{(D)^\top}\mathbf{T}^{(D)}\widetilde{\mathbf{T}}_k\mathbf{H}\dot{\widetilde{\mathbf{T}}}^\top\}}_{\varepsilon_{k,1}}\end{aligned} \tag{2.13}$$

Below the manner of calculation of the components $\varepsilon_{k,2}$, $\varepsilon_{k,0}$, $\varepsilon_{k,1}$ is presented. Assuming that the rotation angles of the frame and the load are small, the matrix $\widetilde{\mathbf{T}}$ can be written as

$$\widetilde{\mathbf{T}} = \begin{bmatrix} 1 & -\psi & \theta & x \\ \psi & 1 & -\varphi & y \\ -\theta & \varphi & 1 & z \\ 0 & 0 & 0 & 1 \end{bmatrix} \tag{2.14}$$

and moreover

$$\widetilde{\mathbf{T}} = \mathbf{I} + \sum_{j=1}^{6}\mathbf{D}_j q_j \tag{2.15}$$

where q_j are suitable elements of vectors $\boldsymbol{q}^{(F)}$ or $\boldsymbol{q}^{(L)}$, and matrices $\mathbf{D}_j$ can be defined:

— for $j = 1,2,3$

$$\mathbf{D}_j = \begin{bmatrix} \mathbf{0} & \boldsymbol{a}_j \\ \mathbf{0} & 0 \end{bmatrix} \tag{2.16}$$

where

$$\boldsymbol{a}_1 = \begin{bmatrix} 1 \\ 0 \\ 0 \end{bmatrix} \qquad \boldsymbol{a}_2 = \begin{bmatrix} 0 \\ 1 \\ 0 \end{bmatrix} \qquad \boldsymbol{a}_3 = \begin{bmatrix} 0 \\ 0 \\ 1 \end{bmatrix}$$

— for $j = 4,5,6$

$$\mathbf{D}_j = \begin{bmatrix} \mathbf{R}_j & \mathbf{0} \\ \mathbf{0} & 0 \end{bmatrix} \tag{2.17}$$

where

$$\mathbf{R}_4 = \begin{bmatrix} 0 & 0 & 0 \\ 0 & 0 & -1 \\ 0 & 1 & 0 \end{bmatrix} \qquad \mathbf{R}_5 = \begin{bmatrix} 0 & 0 & 1 \\ 0 & 0 & 0 \\ -1 & 0 & 0 \end{bmatrix} \qquad \mathbf{R}_6 = \begin{bmatrix} 0 & -1 & 0 \\ 1 & 0 & 0 \\ 0 & 0 & 0 \end{bmatrix}$$

From (2.15), the following relationships occur

$$\dot{\widetilde{\mathbf{T}}} = \sum_{j=1}^{6} \mathbf{D}_j \dot{q}_j \qquad \ddot{\widetilde{\mathbf{T}}} = \sum_{j=1}^{6} \mathbf{D}_j \ddot{q}_j \qquad \widetilde{\mathbf{T}}_k = \frac{\partial \widetilde{\mathbf{T}}}{\partial q_k} = \mathbf{D}_j \tag{2.18}$$

If one uses denotations

$$\mathbf{T}^{(D)} = \begin{bmatrix} \boldsymbol{\Phi}_0 & \mathbf{S}_0 \\ \mathbf{0} & 1 \end{bmatrix} \qquad \dot{\mathbf{T}}^{(D)} = \begin{bmatrix} \boldsymbol{\Phi}_1 & \mathbf{S}_1 \\ \mathbf{0} & 0 \end{bmatrix} \qquad \ddot{\mathbf{T}}^{(D)} = \begin{bmatrix} \boldsymbol{\Phi}_2 & \mathbf{S}_2 \\ \mathbf{0} & 0 \end{bmatrix} \tag{2.19}$$

then

$$\begin{aligned}
\mathbf{T}^{(D)\top}\mathbf{T}^{(D)} &= \begin{bmatrix} \boldsymbol{\Phi}_0^\top & \mathbf{0} \\ \mathbf{S}_0^\top & 1 \end{bmatrix} \begin{bmatrix} \boldsymbol{\Phi}_0 & \mathbf{S}_0 \\ \mathbf{0} & 1 \end{bmatrix} = \begin{bmatrix} \boldsymbol{\Phi}_0^\top \boldsymbol{\Phi}_0 & \boldsymbol{\Phi}_0^\top \mathbf{S}_0 \\ \mathbf{S}_0^\top \boldsymbol{\Phi}_0 & \mathbf{S}_0^\top \mathbf{S}_0 + 1 \end{bmatrix} = \begin{bmatrix} \mathbf{I} & \boldsymbol{\Phi}_0^\top \mathbf{S}_0 \\ \mathbf{S}_0^\top \boldsymbol{\Phi}_0 & \mathbf{S}_0^\top \mathbf{S}_0 + 1 \end{bmatrix} \\
\dot{\mathbf{T}}^{(D)\top}\mathbf{T}^{(D)} &= \begin{bmatrix} \boldsymbol{\Phi}_1^\top & \mathbf{0} \\ \mathbf{S}_1^\top & 0 \end{bmatrix} \begin{bmatrix} \boldsymbol{\Phi}_0 & \mathbf{S}_0 \\ \mathbf{0} & 1 \end{bmatrix} = \begin{bmatrix} \boldsymbol{\Phi}_1^\top \boldsymbol{\Phi}_0 & \boldsymbol{\Phi}_1^\top \mathbf{S}_0 \\ \mathbf{S}_1^\top \boldsymbol{\Phi}_0 & \mathbf{S}_1^\top \mathbf{S}_0 \end{bmatrix} \\
\ddot{\mathbf{T}}^{(D)\top}\mathbf{T}^{(D)} &= \begin{bmatrix} \boldsymbol{\Phi}_2^\top & \mathbf{0} \\ \mathbf{S}_2^\top & 0 \end{bmatrix} \begin{bmatrix} \boldsymbol{\Phi}_0 & \mathbf{S}_0 \\ \mathbf{0} & 1 \end{bmatrix} = \begin{bmatrix} \boldsymbol{\Phi}_2^\top \boldsymbol{\Phi}_0 & \boldsymbol{\Phi}_2^\top \mathbf{S}_0 \\ \mathbf{S}_2^\top \boldsymbol{\Phi}_0 & \mathbf{S}_2^\top \mathbf{S}_0 \end{bmatrix}
\end{aligned} \tag{2.20}$$

The relation $\boldsymbol{\Phi}_0^\top \boldsymbol{\Phi}_0 = \mathbf{I}$ is a consequence of orthogonality of the rotation matrix $\boldsymbol{\Phi}_0$. The matrix $\mathbf{H}$ is defined in the coordinate system where axes of the system are central axes of inertia of the body, so

$$\mathbf{H} = \begin{bmatrix} \mathbf{J} & \mathbf{0} \\ \mathbf{0} & m \end{bmatrix} \tag{2.21}$$

where J_{ij} $(ij = 1,2,3)$ are elements of the matrix $\mathbf{J} = \{J_{ij}\}$ defined by formulae presented inter alia in Wittbrodt *et al.* (2006).

2.2.1. Determination of $\varepsilon_{k,2}$ components

For $k = 1,2,3$

Using (2.15), (2.18) and (2.21), after executing proper multiplications, one obtains

$$\widetilde{\mathbf{T}}_k \mathbf{H} \ddot{\widetilde{\mathbf{T}}}^\top = \begin{bmatrix} \mathbf{0} & \boldsymbol{a}_k \\ \mathbf{0} & 0 \end{bmatrix} \begin{bmatrix} \mathbf{J} & \mathbf{0} \\ \mathbf{0} & m \end{bmatrix} \sum_{j=1}^{6} \mathbf{D}_j^\top \ddot{q}_j = \sum_{j=1}^{3} \ddot{q}_j \begin{bmatrix} m\boldsymbol{a}_k \boldsymbol{a}_j^\top & \mathbf{0} \\ \mathbf{0} & 0 \end{bmatrix} \tag{2.22}$$

and next, taking into account (2.20) and (2.22)

$$\varepsilon_{k,2} = \sum_{j=1}^{3} \ddot{q}_j \mathrm{tr} \left\{ \begin{bmatrix} \mathbf{I} & \boldsymbol{\Phi}_0^\top \mathbf{S}_0 \\ \mathbf{S}_0^\top \boldsymbol{\Phi}_0 & \mathbf{S}_0^\top \mathbf{S}_0 + 1 \end{bmatrix} \begin{bmatrix} m\boldsymbol{a}_k \boldsymbol{a}_j^\top & \mathbf{0} \\ \mathbf{0} & 0 \end{bmatrix} \right\} = \sum_{j=1}^{3} \ddot{q}_j \,\mathrm{tr}\,\{m\boldsymbol{a}_k \boldsymbol{a}_j^\top\} = m\ddot{q}_k \tag{2.23}$$

For $k = 4,5,6$

In this case, again based on (2.15), (2.18) and (2.21), one can calculate

$$\widetilde{\mathbf{T}}_k \mathbf{H} \ddot{\widetilde{\mathbf{T}}}^\top = \begin{bmatrix} \mathbf{R}_k & \mathbf{0} \\ \mathbf{0} & 0 \end{bmatrix} \begin{bmatrix} \mathbf{J} & \mathbf{0} \\ \mathbf{0} & m \end{bmatrix} \sum_{j=1}^{6} \mathbf{D}_j^\top \ddot{q}_j = \sum_{j=4}^{6} \begin{bmatrix} \mathbf{R}_k \mathbf{J} \mathbf{R}_j^\top & \mathbf{0} \\ \mathbf{0} & 0 \end{bmatrix} \ddot{q}_j \tag{2.24}$$

and then

$$\begin{aligned} \varepsilon_{k,2} &= \mathrm{tr} \left\{ \begin{bmatrix} \mathbf{I} & \boldsymbol{\Phi}_0^\top \mathbf{S}_0 \\ \mathbf{S}_0^\top \boldsymbol{\Phi}_0 & \mathbf{S}_0^\top \mathbf{S}_0 + 1 \end{bmatrix} \sum_{j=4}^{6} \begin{bmatrix} \mathbf{R}_k \mathbf{J} \mathbf{R}_j^\top & \mathbf{0} \\ \mathbf{0} & 0 \end{bmatrix} \ddot{q}_j \right\} = \\ &= \sum_{j=4}^{6} \mathrm{tr}\,\{\mathbf{R}_k \mathbf{J} \mathbf{R}_j^\top\} \ddot{q}_j = \sum_{j=4}^{6} \mathrm{tr}\,\{\mathbf{R}_j^\top \mathbf{R}_k \mathbf{J}\} \ddot{q}_j \end{aligned} \tag{2.25}$$

Finally, after making suitable multiplications $\mathbf{R}_j^\top \mathbf{R}_k$, one obtains

$$\begin{aligned} \varepsilon_{4,2} &= (J_{11} + J_{22})\ddot{q}_4 - J_{32}\ddot{q}_5 - J_{31}\ddot{q}_6 \\ \varepsilon_{5,2} &= -J_{23}\ddot{q}_4 + (J_{11} + J_{33})\ddot{q}_5 - J_{21}\ddot{q}_6 \\ \varepsilon_{6,2} &= -J_{13}\ddot{q}_4 - J_{12}\ddot{q}_5 + (J_{22} + J_{33})\ddot{q}_6 \end{aligned} \tag{2.26}$$

2.2.2. Determination of $\varepsilon_{k,0}$ components

Taking into consideration (2.15), (2.18), (2.21) and (2.20), and repeating analogical calculations like above, one can define:
— for $k = 1, 2, 3$

$$\varepsilon_{k,0} = m(\mathbf{S}_2^\top \mathbf{\Phi}_0)_k + \sum_{j=1}^{3} q_j m(\mathbf{\Phi}_2^\top \mathbf{\Phi}_0)_{j,k} \tag{2.27}$$

— for $k = 4, 5, 6$

$$\varepsilon_{k,0} = \operatorname{tr}\{\mathbf{\Phi}_2^\top \mathbf{\Phi}_0 \mathbf{R}_k \mathbf{J}\} + \sum_{j=4}^{6} q_j \operatorname{tr}\{\mathbf{\Phi}_2^\top \mathbf{\Phi}_0 \mathbf{R}_k \mathbf{J} \mathbf{R}_j^\top\} \tag{2.28}$$

2.2.3. Determination of $\varepsilon_{k,1}$ components

Proceeding analogically as for the components $\varepsilon_{k,2}$ and $\varepsilon_{k,0}$, one obtains:
— for $k = 1, 2, 3$

$$\varepsilon_{k,1} = \sum_{j=1}^{3} \dot{q}_j m(\mathbf{\Phi}_1^\top \mathbf{\Phi}_0)_{j,k} \tag{2.29}$$

— for $k = 4, 5, 6$

$$\varepsilon_{k,1} = \sum_{j=4}^{6} \dot{q}_j \operatorname{tr}(\mathbf{\Phi}_1^\top \mathbf{\Phi}_0 \mathbf{R}_k \mathbf{J} \mathbf{R}_j^\top)_{j,k} \tag{2.30}$$

The implementation of relationships (2.23), (2.26), (2.27), (2.28), (2.29) and (2.30) in a computer program describing Lagrange operators in explicit forms instead of general form (2.9), allows one to extremely reduce the calculation time.

The derivatives of the potential energy are gravity forces acting on the element of mass m and they can be presented in the form of a vector

$$\frac{\partial V_g}{\partial \boldsymbol{q}} = [mgt_{31}^{(D)}, mgt_{32}^{(D)}, mgt_{33}^{(D)}, 0, 0, 0]^\top \tag{2.31}$$

where $\boldsymbol{q}$ is the vector of coordinates of the frame or the load (defined in (2.2)), respectively, m – mass of the frame or the load, $t_{31}^{(D)}, t_{33}^{(D)}, t_{33}^{(D)}$ – corresponding elements of the third row of the matrix $\mathbf{T}^{(D)}$.

2.3. Model of the support of BOP crane

It has been assumed that the frame of the BOP crane is supported flexibly in four points denoted as $P^{(k)}$ $(k = 1, 2, 3, 4)$. The crane is moving on a dedicated rail system in the direction parallel to $\widehat{\boldsymbol{X}}^{(D)}$ axis – Fig. 4. Additionally, a constructional clearance can occur in the $\widehat{\boldsymbol{Y}}^{(D)}$ direction.

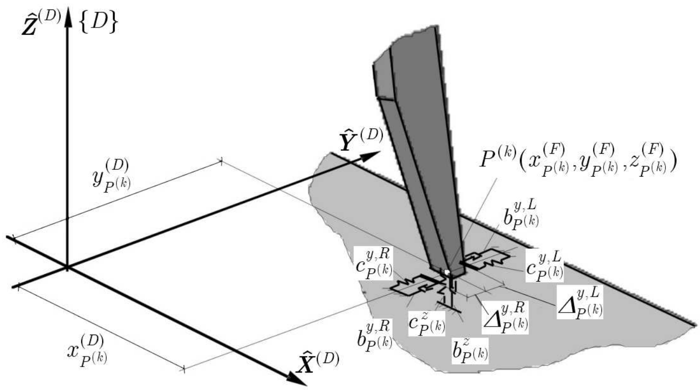

Fig. 4. Flexible connection of the frame to the deck

The reaction force, i.e. the reaction force of the base on the frame, is depicted by the vector

$$\boldsymbol{F}^{(F)}_{P^{(k)}} = [F^{(F,x)}_{P^{(k)}}, F^{(F,y)}_{P^{(k)}}, F^{(F,z)}_{P^{(k)}}]^{\top} \tag{2.32}$$

The $F^{(F,z)}_{P^{(k)}}$ component can be calculated as

$$F^{(F,z)}_{P^{(k)}} = F^{(F,z)}_{S,P^{(k)}} + F^{(F,z)}_{T,P^{(k)}} \tag{2.33}$$

where $F^{(F,z)}_{S,P^{(k)}}$ is the stiffness force and $F^{(F,z)}_{T,P^{(k)}}$ the damping force.

The stiffness and damping forces are determined by relations

$$F^{(F,z)}_{S,P^{(k)}} = -c^{z}_{P^{(k)}} \delta^{z}_{P^{(k)}} \Delta z_{P^{(k)}} \qquad\qquad F^{(F,z)}_{T,P^{(k)}} = -b^{z}_{P^{(k)}} \delta^{z}_{P^{(k)}} \Delta \dot{z}_{P^{(k)}} \tag{2.34}$$

where

$$\delta^{z}_{P^{(k)}} = \begin{cases} 1 & \text{when} \quad \Delta z_{P^{(k)}} < 0 \\ 0 & \text{when} \quad \Delta z_{P^{(k)}} \geqslant 0 \end{cases}$$

and $\Delta z_{P^{(k)}} = z^{(D)}_{P^{(k)}} - z^{(D,0)}_{P^{(k)}}$, where $z^{(D,0)}_{P^{(k)}} = 0$, and $z^{(D)}_{P^{(k)}}$ is the z coordinate of the point $P^{(k)}$ in the system $\{D\}$, $\Delta \dot{z}_{P^{(k)}} = \dot{z}^{(D)}_{P^{(k)}}$, $c^{z}_{P^{(k)}}$, $b^{z}_{P^{(k)}}$ – stiffness and damping coefficients of the connection in the $\widehat{\boldsymbol{Z}}^{(D)}$ direction, respectively.

In the case of the component $F^{(F,y)}_{P^{(k)}}$, the possibility of occurrence of clearance in the anti-lift system is taken into account. To model the clearance, two spring-damping elements acting in the $\widehat{\boldsymbol{Y}}^{(D)}$ direction are introduced. One is the type R element and the second – type L. They are shown in Fig. 4.

The characteristics of force in the spring-damping elements are presented in Fig. 5. They are not linear because of computer implementation (avoidance of discontinuous derivative of the force).

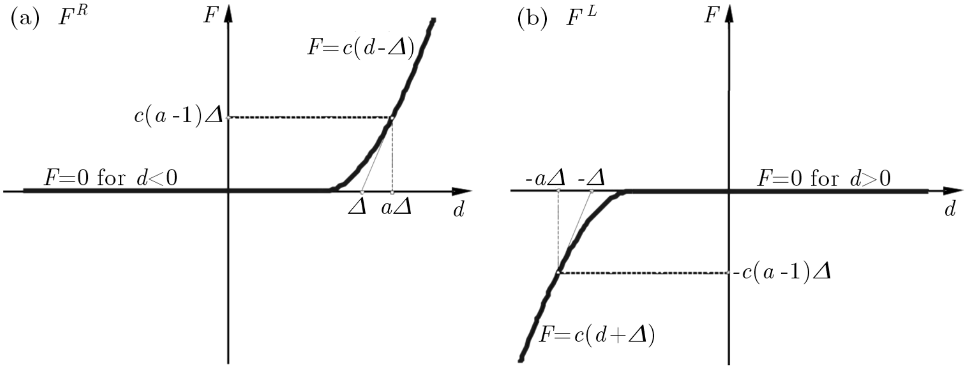

Fig. 5. Characteristics of the force F in the spring-damping element (Δ – clearance, d – deflection of the element), (a) type R, (b) type L

The function describing characteristics given in Fig. 5 can be defined as:
— for the element type R

$$F = \begin{cases} c(d-\Delta) & \text{when} \quad d > a\Delta \\ F^R & \text{when} \quad 0 \leqslant d \leqslant a\Delta \\ 0 & \text{when} \quad d < 0 \end{cases} \tag{2.35}$$

— for the element type L

$$F = \begin{cases} 0 & \text{when} \quad d > 0 \\ F^L & \text{when} \quad -a\Delta \leqslant d \leqslant 0 \\ c(d+\Delta) & \text{when} \quad d \leqslant -a\Delta \end{cases} \tag{2.36}$$

It has been assumed that the functions F^R and F^L have the form

$$F^{(R,L)} = \alpha d^2 e^{\beta d} \tag{2.37}$$

which guarantees the fulfilment of the following conditions

$$F^{(R,L)}(0) = 0 \qquad\qquad F^{(R,L)'}(0) = 0 \tag{2.38}$$

The parameters α, β from (2.37) can be obtained by using conditions:
— for the element type R

$$\begin{aligned} F^R(a\Delta) &= c(a-1)\Delta = F_0^R \\ F^{R'}(a\Delta) &= c = F_0' \end{aligned} \tag{2.39}$$

— for the element type L

$$
\begin{aligned}
F^L(-a\Delta) &= -c(a-1)\Delta = F_0^L \\
F^{L\prime}(-a\Delta) &= c = F_0'
\end{aligned}
\tag{2.40}
$$

Finally, the component $F_{P(k)}^{(F,y)}$ from (2.32) can be presented as:
— for the element type R

$$
F_{P(k)}^{(F,y)} = \begin{cases}
-c_{P(k)}^{y,R}(\Delta y_{P(k)} - \Delta_{P(k)}^{y,R}) - b_{P(k)}^{y,R}\Delta\dot{y}_{P(k)} & \text{when} \quad \Delta y_{P(k)} > a\Delta_{P(k)}^{y,R} \\
F^R & \text{when} \quad 0 \leqslant \Delta y_{P(k)} \leqslant a\Delta_{P(k)}^{y,R} \\
0 & \text{when} \quad \Delta y_{P(k)} < 0
\end{cases}
\tag{2.41}
$$

— for the element type L

$$
F_{P(k)}^{(F,y)} = \begin{cases}
-c_{P(k)}^{y,L}(\Delta y_{P(k)} - \Delta_{P(k)}^{y,L}) - b_{P(k)}^{y,L}\Delta\dot{y}_{P(k)} & \text{when} \quad \Delta y_{P(k)} > 0 \\
F^L & \text{when} \quad -a\Delta_{P(k)}^{y,L} \leqslant \Delta y_{P(k)} \leqslant 0 \\
0 & \text{when} \quad \Delta y_{P(k)} \leqslant -a\Delta_{P(k)}^{y,L}
\end{cases}
\tag{2.42}
$$

where $\Delta y_{P(k)} = y_{P(k)}^{(D)} - y_{P(k)}^{(D,0)}$, $\Delta\dot{y}_{P(k)} = \dot{y}_{P(k)}^{(D)}$, $c_{P(k)}^{y,L}$, $c_{P(k)}^{y,R}$, $b_{P(k)}^{y,L}$, $b_{P(k)}^{y,R}$ is the stiffness and damping coefficients of the connection in the $\widehat{\boldsymbol{Y}}^{(D)}$ direction, respectively.

The component $F_{P(k)}^{(F,x)}$ from (2.32) can be expressed by the formula

$$
F_{P(k)}^{(F,x)} = -\operatorname{sgn}(v_{P(k)}^{(D,x)})S_{P(k)}^{(F,x)}(F_{P(k)}^{(F,y)}, F_{P(k)}^{(F,z)}) \tag{2.43}
$$

where $S_{P(k)}^{(F,x)}$ is the resisting force caused by rolling or sliding friction, $v_{P(k)}^{(D,x)}$ – component x of the velocity of the point $P^{(k)}$ in the coordinate system $\{D\}$.

After calculating suitable coordinates and velocity of points of the support, the generalised force of flexible connection of the frame and deck can be written as

$$
\boldsymbol{Q}_{P(k)}^{(F)} = \mathbf{U}_{P(k)}^{(F)\top} \boldsymbol{F}_{P(k)}^{(F)} \tag{2.44}
$$

where

$$
\mathbf{U}_{P(k)}^{(F)} = \begin{bmatrix}
1 & 0 & 0 & -y_{P(k)}^{(F)} & z_{P(k)}^{(F)} & 0 \\
0 & 1 & 0 & x_{P(k)}^{(F)} & 0 & -z_{P(k)}^{(F)} \\
0 & 0 & 1 & 0 & -x_{P(k)}^{(F)} & y_{P(k)}^{(F)}
\end{bmatrix}
$$

Generalising relation (2.44) to four supports, one can obtain

$$\boldsymbol{Q}_p^{(F)} = \sum_{k=1}^{4} \boldsymbol{Q}_{P^{(k)}}^{(F)} = \sum_{k=1}^{4} \mathbf{U}_{P^{(k)}}^{(F)\;\top} \boldsymbol{F}_{P^{(k)}}^{(F)} \qquad (2.45)$$

2.4. Modelling of the clearance between the load and guides

The guides have been replaced by spring-damping elements (sde) with a clearance (sde $E^{(k,p)}$) that limited the movement of the load in the $\widehat{\boldsymbol{X}}^{(D)}$ and $\widehat{\boldsymbol{Y}}^{(D)}$ directions, see Fig. 6. It has been assumed that the load can contact with guides only along its edges and the number of spring-damping elements can be different for each edge. The manner of calculation of stiffness and damping forces coming from each side is analogical to that one presented in Section 2.3. Additionally, one has to determine equivalent coefficients of flexibility of the elements modelling the guides. Suitable calculations have been executed by means of the finite elements method. They will be presented in details in the doctoral thesis by Urbaś.

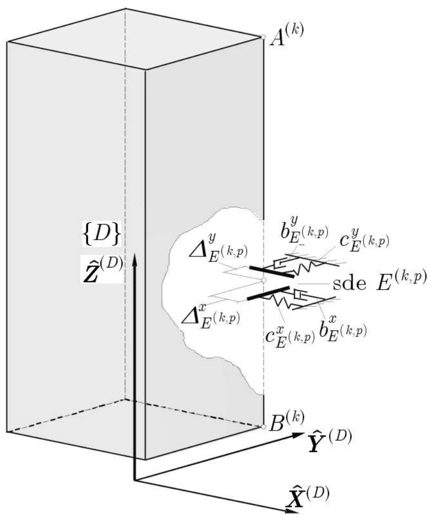

Fig. 6. Load and spring-damping elements with clearance

2.5. The drive of the travel system

The input in the drive of the travel system has been modelled in two ways: kinematic input via a spring-damping element (flexible) and force input (rigid) – Fig. 7. It has been assumed that the drive acts in the points $P^{(1)}$ and $P^{(4)}$.

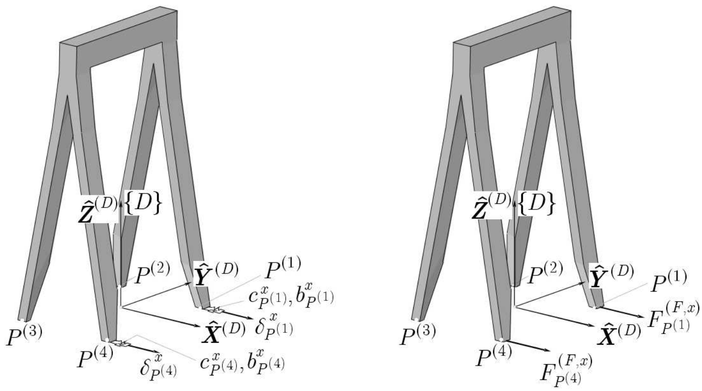

Fig. 7. The travel system of the crane (a) flexible, (b) rigid

2.5.1. Kinematic input

In this case, the potential energy of elastic deformation and the dissipation function of the drive system can be calculated as

$$V_t^{(i)} = \frac{1}{2}c^x_{P(i)}[\delta^x_{P(i)}(t) - x^{(D)}_{P(i)}]^2 \qquad D_t^{(i)} = \frac{1}{2}b^x_{P(i)}[\dot{\delta}^x_{P(i)}(t) - \dot{x}^{(D)}_{P(i)}]^2 \tag{2.46}$$

for $i = 1, 4$, where $\delta^x_{P(1)}(t)$, $\delta^x_{P(4)}(t)$ is the assumed displacement (kinematic input), $c^x_{P(i)}$, $b^x_{P(i)}$ – stiffness and damping coefficients of the drive of the travel system, respectively.

After determining the coordinates $x^{(D)}_{P(i)}$ as functions of elements of the vector $\boldsymbol{q}^{(F)}$, one should place suitable derivatives in the first six equations of motion of system (2.3).

2.5.2. Force input

In this case, the unknown forces $F^{(F)}_{P(1)}$, $F^{(F)}_{P(4)}$ and suitable constraint equations have been introduced. Generally, the forces can be placed on the left-hand side of the equations of motion of the system, which can be written as

$$\mathbf{A}\ddot{\boldsymbol{q}} - \mathbf{D}\boldsymbol{F} = \boldsymbol{f} \tag{2.47}$$

where

$$\mathbf{D} = \begin{bmatrix} \mathbf{0} & \mathbf{0} \\ \mathbf{U}^{(F)}_{P^{(1)},1}{}^{\top} & \mathbf{U}^{(F)}_{P^{(4)},1}{}^{\top} \end{bmatrix} \qquad \boldsymbol{F} = \begin{bmatrix} F^{(F)}_{P(1)} \\ F^{(F)}_{P(4)} \end{bmatrix}$$

$\mathbf{U}^{(F)}_{P^{(1)},1}{}^{\top}$, $\mathbf{U}^{(F)}_{P^{(4)},1}{}^{\top}$ – the first rows of matrices from (2.44).

In the analysed problem the constraint equations have the form

$$x^{(D)}_{P(1)} = \delta^{(D)}_{P(1)}(t) \qquad x^{(D)}_{P(4)} = \delta^{(D)}_{P(4)}(t) \tag{2.48}$$

Because of the convenience of computer implementation, they can be presented in the matrix and acceleration form

$$\mathbf{D}^\top \ddot{\boldsymbol{q}} = \ddot{\boldsymbol{\delta}} = \begin{bmatrix} \delta^{(D)}_{P(1)}(t) \\ \delta^{(D)}_{P(4)}(t) \end{bmatrix} \tag{2.49}$$

2.6. Energy of elastic deformation and energy dissipation in ropes

The load is suspended on two ropes, so their energy of elastic deformation and energy dissipation can be written as

$$V^{(p)}_r = \sum_{p=1}^{2}\Big(\frac{1}{2}c^{(p)}_r \delta^{(p)}_r [\Delta l^{(p)}_{A_pB_p}]^2\Big) \qquad D^{(p)}_r = \sum_{p=1}^{2}\Big(\frac{1}{2}b^{(p)}_r \delta^{(p)}_r [\Delta \dot{l}^{(p)}_{A_pB_p}]^2\Big) \tag{2.50}$$

where $c^{(p)}_r$, $d^{(p)}_r$ are stiffness and damping coefficients of the rope p, respectively, $\Delta l^{(p)}_{A_pB_p}$ – deformation of the rope p, and

$$\delta^{(p)}_r = \begin{cases} 0 & \text{when} \quad \Delta l^{(p)}_{A_pB_p} \leqslant 0 \\ 1 & \text{when} \quad \Delta l^{(p)}_{A_pB_p} > 0 \end{cases}$$

Derivation of formulae defining suitable derivatives of relations (2.50) was presented by Urbaś and Wojciech (2008).

3. Numerical calculations

Taking into consideration all components of Lagrange equations (2.3), a system of differential equations has been obtained

$$\mathbf{A}\ddot{\boldsymbol{q}} = \boldsymbol{f}(t, \boldsymbol{q}, \dot{\boldsymbol{q}}) \tag{3.1}$$

where $\mathbf{A} = \mathbf{A}(t, \boldsymbol{q})$ is the mass matrix.

In the case when the input in the drive of the travel system has been modelled as the force input, equations (3.1) have to be completed by constraint equations (2.49) and the equations of motion have to be presented in form (2.47). The fourth-order Runge-Kutta method has been used to solve the system of equations.

Masses and geometrical parameters have been chosen based upon technical documentation (2007). The main parameters are: mass of the frame 73 955 kg, mass of the load 550 000 kg, dimension of the load $4.8 \times 5.5 \times 20.3$ m. Data concerning the motion of the deck that should be taken into calculation are also provided in Technical documentation (2007), see Table 1. In our simulations, the operational conditions have been assumed.

Table 1. Deck motion due to waves

Condition	Heading [deg]	Heave [m]	Pitch [rad]	Roll [rad]
Z1	0	0.1343	0.0023	0
Z2	45	0.1115	0.0008	0.0023
Z3	90	0.1140	0	0.0045

Calculations for the BOP crane that does not move on the deck have been denoted according to Table 2. The same denotations are used in the graphs.

Table 2. Analysed load cases – gantry crane not moving

Symbol	Description	Clearance	Deck motion
Z1-M0-C0	No clearance in travel system	0	Z1
Z2-M0-C0		0	Z2
Z3-M0-C0		0	Z3
Z1-M0-C1	With clearance in travel system	1cm	Z1
Z2-M0-C1		1cm	Z2
Z3-M0-C1		1cm	Z3

Figure 8 presents time courses of the general coordinates $\psi^{(L)}$ of the load of the BOP crane with and without clearance in the travel system.

The influence of clearance in the travel system on the reaction forces in the support system (leg no. 1) is shown in Fig. 9. The deck motions Z2 and Z3 are taken into consideration.

The biggest influence of clearance in the travel system on the dynamics of the BOP crane occurs for input Z3, so this input is taken into account for the next calculations. The influence of clearance in the travel system on the reaction forces will be analysed. The travel velocity is defined by the relation

$$v = \begin{cases} 3at^2 - 4bt^3 & \text{when} \quad t \leqslant T_r \\ v_n & \text{when} \quad t > T_r \end{cases} \tag{3.2}$$

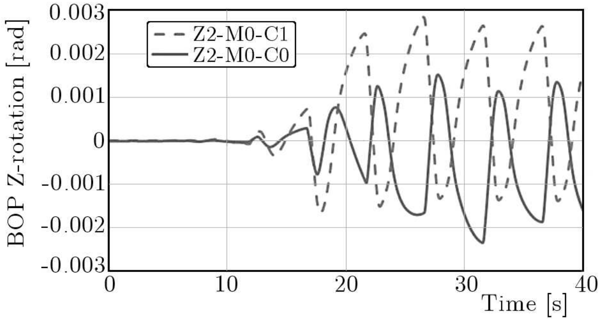

Fig. 8. Influence of clearance on the roll angle of BOP

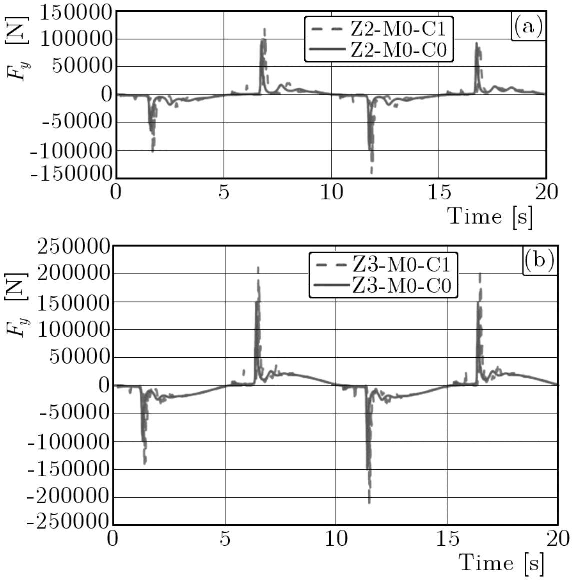

Fig. 9. Lateral reaction in leg no. 1; (a) – in sea conditions Z2, (b) – in sea conditions Z3

where $v_n = 3\,\mathrm{m/min},\ T_r = 6\,\mathrm{s},\ a = v_n/T_r^2,\ b = v_n/(2T_r^3)$.

The left graph in Fig. 10 shows the drive force on the first gear (support no. 1) for the kinematic and force input and for the case when no clearance occurs in the system. The right graph presents the influence of clearance on the drive force. One can notice that the clearance causes the occurrence of significant dynamic forces of short duration.

Required courses of drive forces acting on legs 1 and 4 realising the established travel of the crane are presented in Fig. 11. Kinematic and force inputs have been simulated.

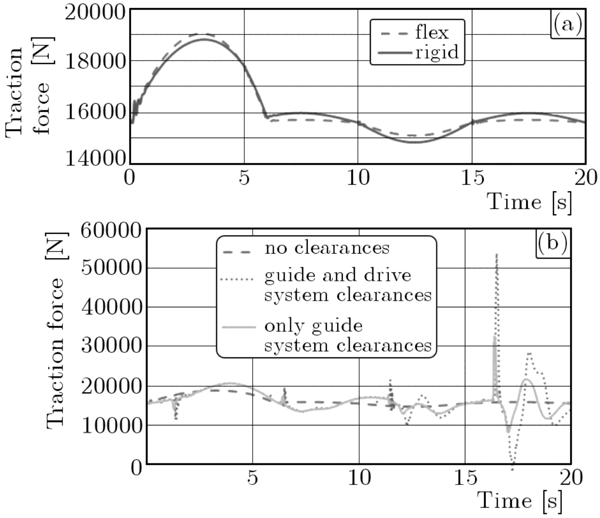

Fig. 10. Drive force on gear no. 1 for the flexible and rigid model applied (a), influence of different clearances on the drive force (b)

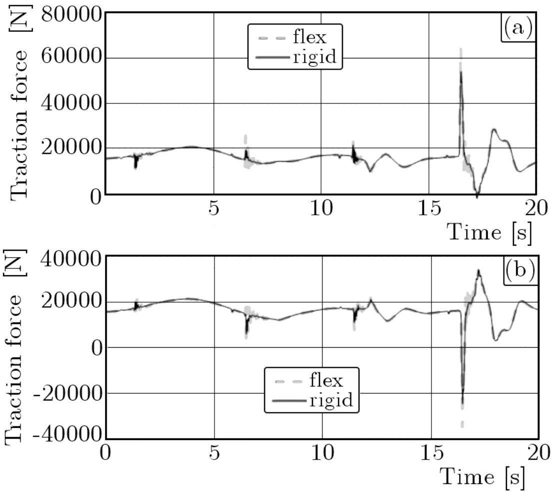

Fig. 11. Rigid and flexible drive, leg no. 1 (a) and no. 4 (b)

The obtained results (values of forces) for the assumed parameters are similar, but for the kinematic input peak values are bigger. These values depend on the stiffness and damping coefficients taken into account during calculations.

For graphs in Fig. 12, the additional clearance of 2 cm in the supporting system for the undrived legs (i.e. 2 and 3) has been taken into consideration.

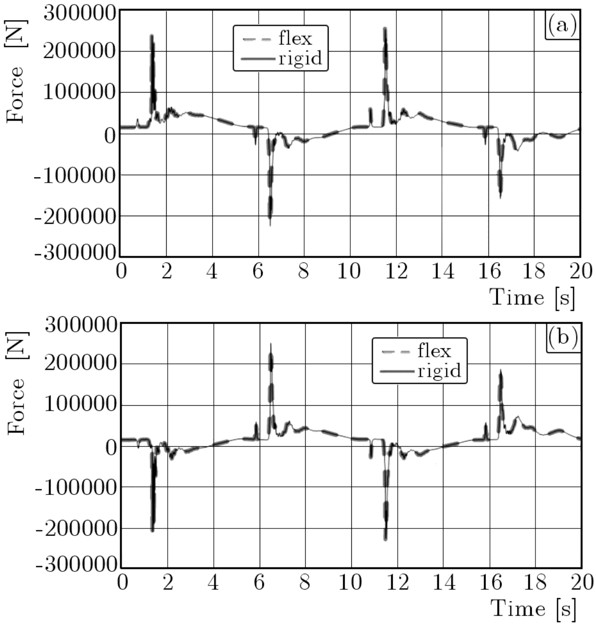

Fig. 12. Rigid and flex drive on leg no. 1 (a) and no. 4 (b) – double size clearance in legs 2 and 3

The obtained values of dynamic forces prove the significant influence of clearance on dynamic load of the drive system, the track-way and the whole structure of the crane.

4. Summary

The mathematical models and the computer programs presented in the paper enable one to execute dynamical analysis of BOP cranes mounted on the floating base. They can be useful in calculating dynamic loads, dimensioning bearing elements of the crane and the track-way. They enable determination of static and dynamic loads by simulation for arbitrarily chosen sea waving conditions.

Special attention has been paid to the influence of clearance in the drive of the crane travel system on characteristics of forces acting in selected elements of the structure. It can be mentioned that for a limited value of clearances they have slight influence on the drive forces. Practically, it is not possible to construct and maintain the track-way with ideal geometry. Dynamic analysis is a good instrument for calculating forces in the system, especially when a bigger clearance appears. It allows one to determine whether the dynamic loads do not transgress the constructional assumptions under given sea waving conditions.

References

1. Adamiec-Wójcik I., Maczyński A., Wojciech S., 2008, *Zastosowanie metody przekształceń jednorodnych w modelowaniu dynamiki urządzeń offshore*, WKŁ, Warsaw
2. Balachandran B., Li Y.Y., Fang C.C., 1999, A mechanical filter concept for control of non-linear crane-load oscillations, *Journal of Sound and Vibrations*, **228**, 651-682
3. Birkeland O., 1998, Knuckle boom combination crane, *3rd International Offshore Cranes Conference Offshore Cranes – Specification, Design, Refurbishment, Safe Operation and Maintenance*, Stavanger, Norway
4. Cosstick H., 1996, The sway today, *Container Management*, 42-43
5. Das S.N., Das S.K., 2005, Mathematical model for coupled roll and yaw motions of a floating body in regular waves under resonant and non-resonant conditions, *Applied Mathematical Modelling*, **29**, 19-34
6. Driscoll F.R., Lueck R., Nahon G.M., 2000, Development and validation of a lumped-mass dynamics model of a deep-sea ROV system, *Applied Ocean Research*, **22**, 169-18
7. Ellermann K., Kreuzer E., 2003, Nonlinear dynamics in the motion of floating cranes, *Multibody System Dynamics*, **9**, 4, 377-387
8. Fałat P., 2004, *Dynamic Analysis of a Sea Crane of an A-frame Type*, Ph.D. Thesis, Bielsko-Biała [in Polish]
9. Fossen T.I., 1994, *Guidance and Control of Ocean Vehicles*, John Wiley and Sons, Chichester, England
10. *Handbook of Offshore Engineering*, 2005, Edited by Chakrabarti S., Elsevier
11. Jordan M.A., Bustamante J.L., 2007, Numerical stability analysis and control of umbilical-ROV systems in one-degree-of-freedom taut-slack condition, *Nonlinear Dynamic*, **49**, 163-191
12. Li Y.Y., Balachandran B., 2001, Analytical study of a system with a mechanical filter, *Journal of Sound and Vibration*, **247**, 633-653
13. Maczyński A., 2005, *Positioning and Stabilization of the Load for Jib Cranes*, University of Bielsko-Biala [in Polish]

14. Maczyński A., Wojciech S., 2003, Dynamics of a mobile crane and optimisation of the slewing motion of its upper structure, *Nonlinear Dynamic*, **32**, 259-290

15. Maczyński A., Wojciech S., 2007, Stabilization of load position for offshore cranes, *Twelfth World Congress in Mechanism and Machine Science*, Besancon, France [electronic document] s. 1-6 [on-line (03.04.2008) http://130.15.85.212/proceedings/ WorldCongress07/articles/article_cd.htm]

16. Maczyński A., Wojciech S., 2008, Wpływ stabilizacji położenia ładunku żurawia typu offshore na zjawisko odciążania i dociążania liny nośnej, *Teoria Maszyn i Mechanizmów*, Wydawnictwo Akademii Techniczno-Humanistycznej w Bielsku-Białej, 135-143

17. Masoud Y.N., 2000, *A Control System for the Reduction of Cargo Pendulation of Ship-Mounted Cranes*, Virginia Polytechnic Institute and State University, Doctoral Thesis, Blacksburg, Virginia, USA

18. Pedrazzi C., Barbieri G., 1998, LARSC: Launch and recovery smart crane for naval ROV handling, *13th European ADAMS Users' Conference*, Paris,

19. *Technical Documentation for BOP*, 2007, PROTEA, Gdańsk-Olesno

20. Urbaś A., Wojciech S., 2008, Dynamic analysis of the gantry crane used transporting BOP, *Proc. VII Conference Telematics, Logistics and Transport Safety*, 311-323

21. Urbaś A., Wojciech S., 2009, Dynamic analysis of the gantry crane used for transporting BOP, *Modeling, Simulation and Control of Nonlinear Engineering Dynamical Systems: State-of-the-Art, Perspectives and Applications*, Springer, 49-59

22. Wittbrodt E., Adamiec-Wójcik I., Wojciech S., 2006, *Dynamics of Flexible Multibody Systems*, Springer

The research has been financed by the ministry of Science and Higher Education (project No. N502 464934).

Analiza jazdy żurawia BOP w warunkach falowania morskiego

Streszczenie

W pracy przedstawiono model matematyczny umożliwiający analizę dynamiczną żurawia BOP w warunkach falowania morskiego. Żuraw BOP stanowi rodzaj suwnicy bramowej. Instalowany jest na platformach wydobywczych i przeznaczony do transportu zespołu zaworów BOP (*Blowout Preventor*). Do najważniejszych czynników wpływających na jego dynamikę należą: ruch podstawy wywołany falowaniem morza, luzy występujące w połączeniu torowiska z suwnicą, uderzenia ładunku o prowadnice oraz znaczna masa ładunku. W celu przeprowadzenia analiz dynamicznych opracowano model obliczeniowy urządzenia uwzględniający powyższe czynniki. Równania ruchu układu sformułowano przy zastosowaniu metody transformacji jednorodnych. W celu poprawy efektywności numerycznej modelu, wykonano przekształcenia umożliwiające przedstawienie równań w sposób jawny. Wymuszenie w układzie napędu jazdy modelowano dwoma sposobami: jako wymuszenie kinematyczne poprzez element sprężysto-tłumiący oraz jako wymuszenie siłowe. Zaprezentowano przykładowe wyniki obliczeń numerycznych.

Manuscript received September 30, 2009; accepted for print January 25, 2010